Semiclassical evidence of a gap in the density of states of chaotic Andreev billiards

Jack Kuipers, Cyril Petitjean, Daniel Waltner, and Klaus Richter
Institut für Theoretische Physik, Universität Regensburg, D-93040 Regensburg, Germany
(Dated: November 14, 2016)

The connection of a superconductor to a chaotic ballistic quantum dot leads to interesting phenomena, most notably the appearance of a hard gap in its excitation spectrum. Here we treat such an Andreev billiard semiclassically where the density of states is expressed in terms of the classical trajectories of electrons (and holes) that leave and return to the superconductor. We show how classical orbit correlations lead to the formation of the hard gap, as predicted by random matrix theory in the limit of negligible Ehrenfest time $\tau_{\rm E}$, and how the influence of a magnetic field or (via a conjecture) a finite $\tau_{\rm E}$ causes the gap to shrink. Furthermore, for intermediate $\tau_{\rm E}$ we predict a second gap below $E=\pi\hbar/2\tau_{\rm E}$ which would presumably be the clearest signature yet of $\tau_{\rm E}$-effects.

PACS numbers: 05.45.Mt,74.45.+c,74.40.+k,03.65.Sq,03.65.Yz

A superconductor (S) in contact with a normal conductor (N) considerably affects its spectral density of quasiparticle excitations: due to Andreev reflection [1] at the NS interface the density of states (DoS) is suppressed closely above the Fermi energy $E_{\rm F}$. This proximity effect is also expected for an 'Andreev billiard' [2], an impurity-free quantum dot attached to a superconductor [3, 4], and has attracted considerable theoretical attention during the last decade (see [5] for a review).

An Andreev billiard has the interesting peculiarity that the suppression of its (mean) DoS crucially depends on whether the dynamics of its classical counterpart is integrable or chaotic: while the DoS vanishes linearly in energy for the integrable case, the spectrum of a chaotic billiard is expected to exhibit a true gap above $E_{\rm F}$ [6]. Based on random matrix theory (RMT) this gap was predicted to scale with the Thouless energy, $E_{\rm T}=\hbar/2\tau_{\rm D}$, where $\tau_{\rm D}$ is the average (classical) dwell time a particle stays in the billiard between successive Andreev reflections [6]. On the contrary, semiclassics based on the so-called Bohr-Sommerfeld (BS) approximation yields only an exponential suppression of the DoS [7, 8, 9], a discrepancy that has attracted much theoretical interest [10, 11, 12, 13, 14]. Lodder and Nazarov [7] pointed out that these seemingly contradictory predictions are valid in different limits, governed by the ratio $\tau=\tau_{\rm E}/\tau_{\rm D}$. Here the (quantum mechanical) Ehrenfest time $\tau_{\rm E}\sim|\ln\hbar|$ separates the evolution of wave packets following essentially the classical dynamics from longer time scales dominated by wave interference. In the universal regime, $\tau=0$, the Thouless gap (from RMT) is clearly established [6, 10], while the BS approximation describes the classical limit $\tau\to\infty$.

Various approaches have been used to better understand the crossover from the Thouless to the Ehrenfest regime of large τ, where RMT loses its applicability [10]. These include effective RMT [12], predicting a gap size scaling with the Ehrenfest energy $E_{\rm E}=\hbar/2\tau_{\rm E}$, as well as stochastic [13] and perturbative [11] methods. Recently the gap at $\pi E_{\rm E}$ was derived for $\tau\gg1$ in a quasiclassical approach based on the Eilenberger equation [14].

The purpose of this Letter is twofold. Firstly, using the scattering approach [15], we demonstrate that the DoS can be evaluated semiclassically for $\tau_{\rm E}=0$ by using an energy-dependent generalization of the work [16] on the moments of the transmission eigenvalues. This semiclassically computed DoS yields a hard gap, in agreement with RMT. Secondly we address the whole crossover regime of $\tau>0$, in which the Ehrenfest time dependence is incorporated by the means of an Ansatz. Based on this, in the limit $\tau\gg1$, the width of the gap approaches $\pi E_{\rm E}$, eventually recovering the BS prediction for $\tau\to\infty$. More interestingly in the intermediate regime $\tau\geq1$ we predict the appearance of a second 'Ehrenfest' gap at $\pi E_{\rm E}$.

Andreev billiard. In the scattering approach the superconductor is represented by a lead that carries M scattering channels, and the excitation spectrum can be entirely expressed in terms of the (electron) scattering matrix S [15]. The average DoS reads [9] (when divided by twice the average density of the isolated billiard),

$$d(\epsilon)=1+2\sum_{n=1}^{\infty}\frac{(-1)^n}{n}{\rm Im}\frac{\partial C(\epsilon,n)}{\partial\epsilon}, \qquad (1)$$

in terms of correlation functions of n S-matrices,

$$C(\epsilon,n)=\frac{1}{M}{\rm Tr}\left[S^\dagger\left(E_{\rm F}-\frac{\epsilon\hbar}{2\tau_{\rm D}}\right)S\left(E_{\rm F}+\frac{\epsilon\hbar}{2\tau_{\rm D}}\right)\right]^n, \qquad (2)$$

at different energies. Here the energy difference $2E$ is expressed in units of the Thouless energy and $\tau_{\rm D}=T_{\rm H}/M$ with $T_{\rm H}$ the Heisenberg time, *i.e.* the time conjugate to the mean level spacing. For $\epsilon=0$, the $C(\epsilon,n)$ in Eq. (2), when limited to transmission matrices, give the moments of the transmission eigenvalues which were calculated semiclassically (to leading order in M^{-1}) in [16].

Semiclassical evaluation in the universal regime. To evaluate Eq. (2), we start with the semiclassical approximation to the scattering matrix elements connecting the

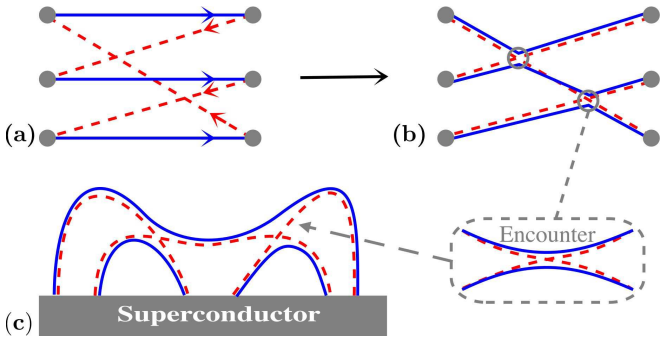

Figure 1: (a) Schematic picture of the trajectory structures for $n=3$. The blue solid lines represent electrons which are retro-reflected as holes (red dashed lines). (b) Collapsing the trajectories onto each other leads to encounters. (c) The end result, *i.e.* correlated Andreev reflected paths.

channel a to b, which are given by [17]

$$S_{ba}(E_{\rm F}\pm E)\approx\frac{1}{\sqrt{T_{\rm H}}}\sum_{\zeta(a\to b)}A_\zeta {\rm e}^{\frac{\rm i}{\hbar}S_\zeta(E_{\rm F}\pm E)}, \qquad (3)$$

in terms of the classical trajectories ζ connecting a to b. Here S_ζ is the action of ζ, and A_ζ is its stability (including Maslov indices). We substitute Eq. (3) into Eq. (2), and expand the action up to first order in the energy yielding the duration $T_\zeta=\partial S_\zeta/\partial E_{\rm F}$. The correlators are then given by a sum over $2n$ trajectories

$$C(\epsilon,n)\approx\frac{1}{M{T_{\rm H}}^n}\prod_{j=1}^{n}\sum_{a_j,b_j}\sum_{\zeta_j(a_j\to b_j)}\sum_{\zeta'_j(b_j\to a_{j+1})} \qquad (4)$$
$$A_{\zeta_j}A^*_{\zeta'_j}\exp\left[({\rm i}/\hbar)(S_{\zeta_j}-S_{\zeta'_j})\right]\exp\left[({\rm i}\epsilon/2\tau_{\rm D})(T_{\zeta_j}+T_{\zeta'_j})\right],$$

with $a_{n+1}=a_1$. The final trace of the product of matrices means that the trajectories complete a cycle, moving forward along the unprimed trajectories and back along the primed ones; an example of this structure for $n=3$ is shown in Fig. 1a. In Eq. (4) we add the actions of all the unprimed trajectories and subtract the actions of the primed ones, so the resulting phase oscillates wildly, unless the total action difference is of the order of $\hbar$. One way to get small action differences is to collapse all the trajectories onto each other, see Fig. 1b. This leads to encounters where the electron trajectories avoid crossing while the hole trajectories cross (or vice versa) to ensure that they each connect the correct channels. Besides this direct collapse further possibilities arise from sliding the encounters together or into the leads, see [16].

But for each possibility we also need to know its semiclassical contribution. Starting for open systems with the treatment of the first off-diagonal pair by [18], the generalization to all orders [19] led to diagrammatic rules, whereby each link (*i.e.* each trajectory stretch connecting channels or encounters) essentially gives a factor of $[M(1-{\rm i}\epsilon)]^{-1}$, while each l-encounter (which involves l electron trajectory stretches) contributes $-M(1-{\rm i}l\epsilon)$ as the stretches are so close that they all remain or escape together. Summing the contributions, by extending the work of [16] to include energy differences, and leaving the technical details to elsewhere, we arrive at the intermediate generating function $g(\epsilon,r)$, which includes all possible diagrams apart from where the top encounter enters the lead. This is given implicitly by the cubic equation

$$g-\frac{1}{(1-{\rm i}\epsilon)}=\frac{rg^2}{(1-{\rm i}\epsilon)}\left[g-\frac{1}{(1-{\rm i}\epsilon)}-\frac{\epsilon^2}{(1-{\rm i}\epsilon)}\right]. \qquad (5)$$

Including the possibility where the top encounter can enter the lead, leads to the generating function

$$G(\epsilon,r)=\frac{g}{1-rg}=C(\epsilon,1)+rC(\epsilon,2)+r^2C(\epsilon,3)+\ldots \qquad (6)$$

of the correlation functions. By inverting (6) we can see that G is also given implicitly by a cubic equation. Expanding G (or g) as a power series in r, we obtain the first few correlation functions (which can be checked by considering the semiclassical diagrams explicitly) as:

$$\begin{aligned} C(\epsilon,1) &= \frac{1}{(1-{\rm i}\epsilon)}, \quad C(\epsilon,2)=\frac{1-2{\rm i}\epsilon-2\epsilon^2}{(1-{\rm i}\epsilon)^4} \\ C(\epsilon,3) &= \frac{1-4{\rm i}\epsilon-9\epsilon^2+8{\rm i}\epsilon^3+5\epsilon^4}{(1-{\rm i}\epsilon)^7} \end{aligned} \qquad (7)$$

Density of states in the universal regime. In view of Eq. (6), the average DoS is given semiclassically by

$$d(\epsilon)=1+2\,{\rm Im}\int {\rm d}r\,\frac{\partial G(\epsilon,r)}{\partial\epsilon}\Big|_{r=-1}. \qquad (8)$$

Though as we have not yet been able to obtain a closed form result for Eq. (8), we generate the correlation functions recursively to obtain a truncated version of the sum in Eq. (1). We choose the following truncation

$$d_m(\epsilon)=1+2\sum_{n=1}^{m-1}\frac{(-1)^n}{n}{\rm Im}\frac{\partial C(\epsilon,n)}{\partial\epsilon}+\frac{(-1)^m}{m}{\rm Im}\frac{\partial C(\epsilon,m)}{\partial\epsilon} \qquad (9)$$

which avoids a semiclassical oscillation at $\epsilon=0$. The DoS (9) can then be compared to the RMT result [6]

$$d_{\rm RMT}(\epsilon)=\sqrt{3}/(6\epsilon)\left[Q_+(\epsilon)-Q_-(\epsilon)\right],\ \epsilon>2[(\sqrt{5}-1)/2]^{\frac{5}{2}} \qquad (10)$$

where $Q_\pm(\epsilon)=\left[8-36\epsilon^2\pm3\epsilon\sqrt{3\epsilon^4+132\epsilon^2-48}\right]^{\frac{1}{3}}$.

In Fig. 2 we plot this DoS against the 120th order result obtained semiclassically from Eq. (9), and we find remarkable agreement. In particular, the gap in the DoS can clearly be seen, and this provides the first semiclassical evidence of the appearance of the RMT gap given by $0.6E_{\rm T}$. We study convergence to the RMT result, by considering $\Delta_m^2=\int_0^\infty\left[d_m(\epsilon)-d_{\rm RMT}(\epsilon)\right]^2{\rm d}\epsilon$. Δ_m^{-1} can be evaluated numerically and follows a straight line very

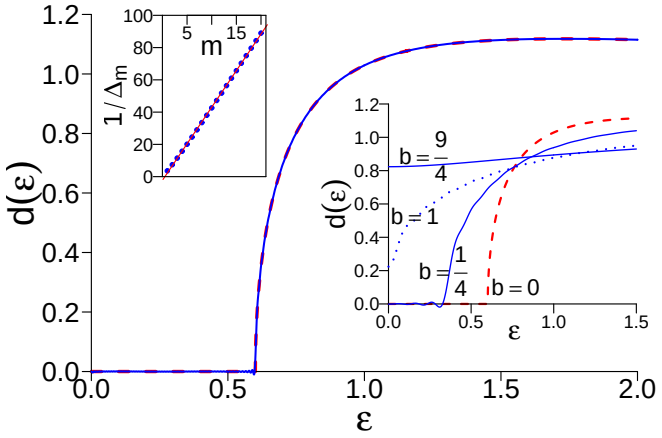

Figure 2: Density of states of a chaotic Andreev billiard: Comparison between semiclassics, Eq. (9) truncated at the 120th order term (full blue line), and RMT, Eq. (10) (dashed red). The top inset shows the inverse difference between the truncated semiclassical and the full RMT result as a function of the order m of truncation, along with a linear fit line. The lower inset shows the effect of a magnetic field.

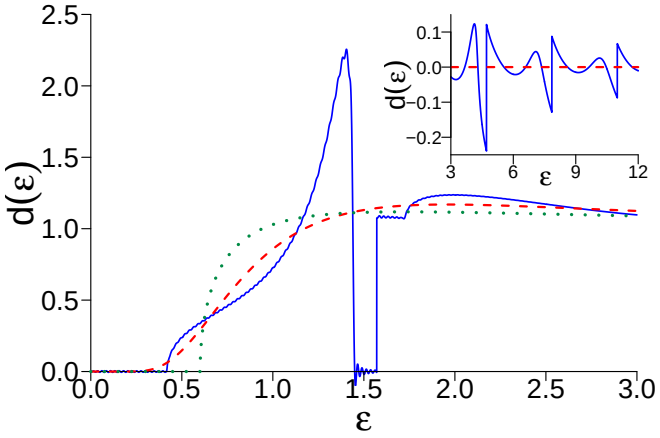

Figure 3: Density of states for $\tau = \tau_{\rm E}/\tau_{\rm D} = 2$ (full line), along with the BS (dashed) and RMT (dotted) limits, showing a second gap just below $\epsilon = \frac{\pi}{2}$. Inset: $\tau_{\rm E}$-related π-periodic DoS oscillations at higher energy (after subtracting the BS curve).

closely, see inset in Fig. 2, along with the linear fit line $\Delta_m^{-1} \approx 4.53m - 2.28$, which suggests that the semiclassical result would eventually converge to the RMT limit.

Magnetic field. A symmetry breaking B-field affects the phases of the paths in an essentially random way, and as each stretch is traversed in opposite directions by an electron and a hole, for the leading order diagrams, we are effectively considering parametric correlations [20, 21]. The random fluctuations add up to lead to an exponential damping of the links, so that each link now provides a factor of $[M(1 - \mathrm{i}\epsilon + b)]^{-1}$, where $b = (\Phi/\Phi_{\rm c})^2$ with $\Phi_{\rm c}$ the critical flux [5]. For an l-encounter however, as the stretches are correlated and affected by the B-field in the same way, the variance of the fluctuations of all the stretches is l^2 that of a single stretch, so each encounter gives a factor $-M(1 - \mathrm{i}l\epsilon + l^2 b)$. This small classical correlation leads to a significant semiclassical effect and to the implicit equation

$$\left(g - \frac{1}{(1 - \mathrm{i}\epsilon + b)} - \frac{rg^2}{(1 - \mathrm{i}\epsilon + b)}\left[g + \frac{(b - \mathrm{i}\epsilon)^2 - 1}{(1 - \mathrm{i}\epsilon)}\right]\right) \times \left(1 - rg^2\right) = -\frac{2brg^3\,(1 - rg)}{(1 - \mathrm{i}\epsilon + b)}\,. \tag{11}$$

Expanding in a power series in r and substituting into (6) we obtain the DoS (9) which we plot for various values of b in the right inset in Fig. 2. These curves very closely mimic the corresponding RMT results in [22].

Density of states in the Ehrenfest regime. The effect of a finite Ehrenfest time $\tau_{\rm E}$ on the first three correlation functions $C(\epsilon, \tau, n)$ with $\tau = \tau_{\rm E}/\tau_{\rm D}$ has previously been calculated semiclassically [23]. For these, the effect of increasing τ_E is twofold; first as each encounter typically lasts an Ehrenfest time forming the diagrams considered before becomes less likely, while conversely the possibility that all the trajectories are correlated for their whole length increases (cf the bands in [14]), and we need to add this additional set of diagrams. As yet the τ_E contributions and the combinatorial rules governing them have not been generalized, but this separation into two classes seems robust. Thus we propose the Ansatz

$$C(\epsilon, \tau, n) = C(\epsilon, n)\mathrm{e}^{-\tau(1 - \mathrm{i}n\epsilon)} + \frac{1 - \mathrm{e}^{-\tau(1 - \mathrm{i}n\epsilon)}}{1 - \mathrm{i}n\epsilon} \tag{12}$$

though we stress that this replacement is only known to be exact for $n \le 3$. Equation (12) reproduces the two known limits: the previous RMT result for $\tau = 0$, and the BS result [8, 9], $d_{\rm BS}(\epsilon) = \left(\frac{\pi}{\epsilon}\right)^2 \frac{\cosh(\pi/\epsilon)}{\sinh^2(\pi/\epsilon)}$, for $\tau = \infty$. Alongside the two limits, this Ansatz, and in particular the $n\epsilon$ dependence in the exponent, leads to interesting $\tau_{\rm E}$-effects: a re-normalized gap and an oscillatory DoS with spikes with period $2\pi/\tau$ giving rise to another gap.

To study this behavior, we substitute Eq. (12) into Eq. (1) and get two contributions, from the two terms. The first yields a reduced RMT-type contribution that can be investigated as before with the help of the truncated DoS (9), while the second contribution can be summed exactly via Poisson summation and reads

$$1 + 2\sum_{n=1}^{\infty} \frac{(-1)^n}{n} \mathrm{Im} \frac{\partial}{\partial \epsilon}\left[\frac{1 - \mathrm{e}^{-\tau(1 - \mathrm{i}n\epsilon)}}{1 - \mathrm{i}n\epsilon}\right] \tag{13}$$
$$= d_{\rm BS}(\epsilon) + \mathrm{e}^{-\tau}\,(1 + \tau) - \mathrm{e}^{-\frac{2\pi k}{\epsilon}}\left[d_{\rm BS}(\epsilon) + \frac{2k\,(\pi/\epsilon)^2}{\sinh\,(\pi/\epsilon)}\right],$$

where $k = \lfloor \frac{\epsilon\tau + \pi}{2\pi} \rfloor$ involving the floor function. We note that this function is constant ($= (1 + \tau)\,\mathrm{e}^{-\tau}$) up to $\epsilon\tau = \pi$ and for $\tau \to \infty$ at fixed $\epsilon\tau$, this contribution leads to a hard gap up to $\pi E_{\rm E}$ in agreement with the recent complementary quasiclassical work of [14].

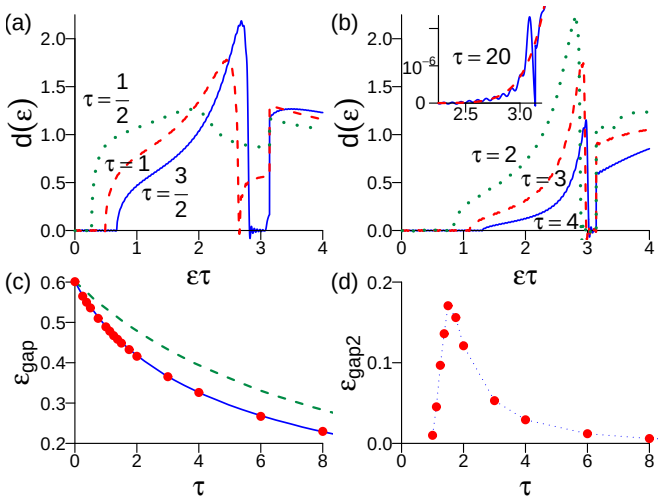

Figure 4: (a,b) Density of states as a function of $\epsilon\tau = E/E_{\rm E}$ for various values of τ showing the appearance of a second gap below $\epsilon\tau = \pi$. Inset: DoS for $\tau = 20$ (full line) together with the BS limit (dashed). (c) Size of the original gap as a function of τ. Our semiclassical results (points) agree with effective RMT [12] (solid line); dashed line: prediction from the stochastic model of [13]. (d) Size of the second gap as a function of τ (dotted line is a guide to the eye).

As an illustration we plot the DoS for $\tau = 2$ in Fig. 3, truncating again at $m = 120$. We find a clear reduction of the RMT gap and in the inset an oscillatory behavior of the DoS at larger energy. We note that $\tau_{\rm E}$-oscillations have previously been predicted [11, 13], however those appearing here have a larger magnitude. More interestingly though, the result in Fig. 3 shows the appearance of a second pronounced gap. More generally, in the regime $1 \leq \tau \lesssim 20$, the DoS contribution stemming from the first term in Eq. (12) increases after the end of the first gap before falling again to lead to the creation of the second gap which ends at the first spike at $\epsilon\tau = E/E_{\rm E} = \pi$ (for $\tau > 3/2$). This structure in the DoS would be a clear-cut signature of the Ehrenfest time. The absence of such a feature in previous numerical work is presumably due to the difficulty in reaching the limit $\tau \geq 1$.

In Fig. 4a, b we show the DoS for different values of τ, illustrating the formation and then the shrinking of the second gap, while the first gap approaches $\epsilon\tau = \pi$, *i.e.* $E = \pi E_{\rm E}$ for $\tau \gg 1$. In panel c we extracted the value of the edge of the first gap. We find agreement with the effective RMT prediction [12], and seem to be in accordance with previous numerical findings [24, 25] limited to $\tau < 1$. Finally in panel d we show the size of the second gap, which forms quickly as τ increases from 1 to 3/2 before slowly shrinking again for larger τ.

Conclusions. Based on a systematic semiclassical treatment of correlation functions involving n scattering matrices, we calculated the density of states of an Andreev billiard semiclassically, and recover a hard gap extending up to $0.6E_{\rm T}$ as in RMT. Likewise, increasing $\tau_{\rm E}$, through the means of a conjecture on its semiclassical contributions, we can see how the gap closes (approaching $E = \pi E_{\rm E}$) in agreement with effective RMT, and we can study the full crossover from the RMT limit (at $\tau_{\rm E} = 0$) to $\tau_{\rm E} \gg \tau_{\rm D}$. Interestingly this transition is not smooth, and inbetween we see the formation of a second gap at $E \simeq \pi E_{\rm E}$ for $\tau_{\rm E} \simeq \tau_{\rm D}$. Such a striking feature, if confirmed, should be an easier $\tau_{\rm E}$-signature to observe experimentally than the change in size of the original gap. In particular we hope this result will add an extra incentive to look at generalizing the semiclassical picture of Ehrenfest time effects to all orders and to see whether our conjecture - and its implications for the density of states of chaotic Andreev billiards - holds true.

We thank İ. Adagideli, A. Altland, G. Berkolaiko, Ph. Jacquod, M. Novaes, C. Strunk, J.D. Urbina, and R.S. Whitney for valuable discussions. We acknowledge funding from the DFG under GRK 638 (DW, KR) and from the Alexander von Humboldt foundation (JK, CP).

[1] A. F. Andreev, Sov. Phys. JETP **19**, 1228 (1964).
[2] I. Kosztin, D. L. Maslov, and P. M. Goldbart, Phys. Rev. Lett. **75**, 1735 (1995).
[3] A. F. Morpurgo et al., Phys. Rev. Lett. **78**, 2636 (1997).
[4] M. Jakob et al., App. Phys. Lett. **76**, 1152 (2000).
[5] C. W. J. Beenakker, Lect. Notes Phys. **667**, 131 (2005).
[6] J. A. Melsen, P. W. Brouwer, K. M. Frahm, and C. W. J. Beenakker, Europhys. Lett. **35**, 7 (1996).
[7] A. Lodder and Y. V. Nazarov, Phys. Rev. B **58**, 5783 (1998).
[8] H. Schomerus and C. W. J. Beenakker, Phys. Rev. Lett. **82**, 2951 (1999).
[9] W. Ihra, M. Leadbeater, J. L. Vega, and K. Richter, Eur. Phys. J. B **29**, 425 (1995).
[10] D. Taras-Semchuk and A. Altland, Phys. Rev. B **64**, 014512 (2001).
[11] İ. Adagideli and C. W. J. Beenakker, Phys. Rev. Lett. **89**, 237002 (2002).
[12] P. G. Silvestrov, M. C. Goorden, and C. W. J. Beenakker, Phys. Rev. Lett. **90**, 116801 (2003).
[13] M. G. Vavilov and A. I. Larkin, Phys. Rev. B **67**, 115335 (2003).
[14] T. Micklitz and A. Altland (2009), arXiv:0901.3137v1, and private communication.
[15] C. W. J. Beenakker, Phys. Rev. Lett. **67**, 3836 (1991).
[16] G. Berkolaiko, J. M. Harrison, and M. Novaes, J. Phys. A **41**, 365102 (2008).
[17] W. H. Miller, Adv. Chem. Phys. **30**, 77 (1975).
[18] K. Richter and M. Sieber, Phys. Rev. Lett. **89**, 206801 (2002).
[19] S. Heusler, S. Müller, P. Braun, and F. Haake, Phys. Rev. Lett. **96**, 066804 (2006).
[20] T. Nagao et al., J. Phys. A **40**, 47 (2007).
[21] J. Kuipers and M. Sieber, J. Phys. A **40**, 935 (2007).
[22] J. A. Melsen, P. W. Brouwer, K. M. Frahm, and C. W. J. Beenakker, Phys. Scr. **T69**, 223 (1997).

[23] P. W. Brouwer and S. Rahav, Phys. Rev. B **74**, 085313 (2006).
[24] Ph. Jacquod, H. Schomerus, and C. W. J. Beenakker, Phys. Rev. Lett. **90**, 207004 (2003).
[25] A. Kormányos, Z. Kaufmann, C. J. Lambert, and J. Cserti, Phys. Rev. B **70**, 052512 (2004).